Bioorganic & Medicinal Chemistry 20 (2012) 3799–3806

Contents lists available at SciVerse ScienceDirect

Bioorganic & Medicinal Chemistry

journal homepage: www.elsevier.com/locate/bmc

Protuboxepin A, a marine fungal metabolite, inducing metaphase arrest and chromosomal misalignment in tumor cells

Yukihiro Asami [a,b,†], Jae-Hyuk Jang [a,†], Nak-Kyun Soung [a,c], Long He [a], Dong Oh Moon [d], Jong Won Kim [a], Hyuncheol Oh [e], Makoto Muroi [b], Hiroyuki Osada [b], Bo Yeon Kim [a,c,*], Jong Seog Ahn [a,*]

[a] Chemical Biology Research Center, Korea Research Institute of Bioscience and Biotechnology (KRIBB), 30 Yeongudanji-ro, Ochang, Cheongwon, Chungbuk 363-883, Republic of Korea
[b] Chemical Biology Department, RIKEN Advanced Science Institute, 2-1 Hirosawa, Wako-shi, Saitama 351-0198, Japan
[c] World Class Institute, (KRIBB), 30 Yeongudanji-ro, Ochang, Cheongwon, Chungbuk 363-883, Republic of Korea
[d] Department of Biology Education, Daegu University, Jillyang, Gyeongsan, Gyeongbuk 712-714, Republic of Korea
[e] College of Pharmacy, Wonkwang University, Iksan 570-749, Republic of Korea

ARTICLE INFO

Article history:
Received 22 March 2012
Revised 19 April 2012
Accepted 19 April 2012
Available online 27 April 2012

Keywords:
Protuboxepin A
Marine fungal metabolite
Metaphase arrest
Chromosomal misalignment
Tubulin

ABSTRACT

Previously we reported the identification of a new oxepin-containing diketopiperazine-type marine fungal metabolite, named protuboxepin A which showed antiproliferative activity in several cancer cell lines. In this study we elucidated the mechanism by which protuboxepin A induces cancer cell growth inhibition. Here we report that protuboxepin A induced round-up morphology, M phase arrest, and an increase in the subG$_1$ population in tumor cells in a dose dependent manner. Our investigations revealed that protuboxepin A directly binds to α,β-tubulin and stabilizes tubulin polymerization thus disrupting microtubule dynamics. This disruption leads to chromosome misalignment and metaphase arrest which induces apoptosis in cancer. Overall, we identified protuboxepin A as a microtubule-stabilizing agent which has a distinctly different chemical structure from previously reported microtubule inhibitors. These results indicate that protuboxepin A has a potential of being a new and effective anti-cancer drug.

1. Introduction

Cancer is a leading cause of death in the world. Some of the most effective anti-tumor drugs target microtubule dynamics.[1–5] Two classes of these drugs, the taxanes, (taxol/paclitaxel and docetaxel/taxotere) and the *vinca* alkaloids (vindesine, vinorelbine, and vinflunine), have received FDA approval and have been used in clinical trials in which they were shown to increase the remission rates of a number of cancers such as advanced ovarian cancer, metastatic breast cancer, and lung cancer.[6–10] The taxanes and *vinca* alkaloids are known as mitotic inhibitors because they interfere with the function of the mitotic spindle inducing mitotic arrest and apoptosis.[11] The mitotic spindle plays an important role in a variety of cellular processes that influence cell shape and organization, as well as chromosome segregation during mitosis.[12] Spindle function is dependent on microtubule dynamics, which involves the stochastic gain and loss of α- and β-tubulin heterodimers from microtubule ends. The taxanes and *vinca* alkaloids inhibit microtubules thereby interfering with the normal breakdown of microtubules during cell division. Although these mitotic inhibitors are useful chemotherapy drugs for many cancers, they are still ineffective against several solid tumor cancers such as kidney, pancreas, or colon carcinomas.[5,8] In addition many cancers eventually develop resistance to these drugs. For these reasons, there is an urgent need to identify novel tubulin inhibitors that can be developed into new cancer therapy drugs.[13,14] In 2010, E7389 (Halaven™), a macrocyclic ketone analog of the marine natural product halichondrin B, was approved by FDA as a novel anti-cancer drug.[14] This fully synthetic agent exerts its highly potent in vitro and in vivo anti-cancer effects via tubulin-based anti-mitotic mechanisms.[15–19]

In a previous study, we reported the identification a new oxepin-containing diketopiperazine-type compound, named protuboxepin A that displayed antiproliferative activity against several cancer cell lines. The mechanism by which protuboxepin A inhibited tumor cell growth was unknown (Fig. S1 and S2). [20] In this study, we reveal that protuboxepin A exerts its effect by inhibiting microtubule dynamics through the tubulin polymerizing. Protuboxepin A binds to α, β-tubulin heterodimers and accelerates tubulin polymerization in vitro resulting in chromosome misalignment and metaphase arrest which leads to apoptosis in tumor cells.

* Corresponding authors. Tel.: +82 43 240 6163; fax: +82 43 240 6169 (B.Y.K.); tel.: +82 43 240 6164; fax: +82 43 240 6169 (J.S.A.).
E-mail addresses: bykim@kribb.re.kr (B.Y. Kim), jsahn@kribb.re.kr (J.S. Ahn).
† These authors contributed equally to this work.

0968-0896/$ - see front matter Crown Copyright © 2012 Published by Elsevier Ltd. All rights reserved.
http://dx.doi.org/10.1016/j.bmc.2012.04.039

2. Results and discussion

2.1. Effects of protuboxepin A on tumor cells

Protuboxepin A induced round-up morphology and increased subG$_1$ and G$_2$/M phase populations in Hep3B and MDA-MB-231cells in a dose-dependent manner at 24 and 48 h, respectively (Figs. 1A–C and S3). The mechanism by which protuboxepin A caused these biological effects was investigated. Since protuboxepin A showed a similar phenotype as tubulin inhibitors, such as nocodazole and paclitaxel we hypothesized that protuboxepin A may also inhibit tubulin function. To confirm this hypothesis, we compared protuboxepin A activity to that of paclitaxel, a known microtubule-stabilizing agent. Western blot analysis of Hep3B cells showed that protuboxepin A, at a 160 μM level, induced phosphorylation of Bcl-2 (Ser70) and decreased phosphorylation of cdc2 (Tyr15) after a 18 h. Figure 1D shows that protuboxepin A is far less potent than paclitaxel. In addition, both protuboxepin A and paclitaxel induced caspase-3 and PARP cleavage (Fig. 1E) which are apoptotic markers. These results are consistent with known tubulin inhibitors which induce Bcl-2 phosphorylation at Ser70, decrease cdc2 phosphorylation at Tyr15 and eventually causes apoptosis in tumor cell.[21–24] In addition, FUCCI (Fluorescent Ubiquitination-based Cell Cycle Indicator) analysis of HeLa cells revealed that protuboxepin A, at a 160 μM level, up-regulated the G$_2$/M maker geminin-GFP (Fig. 1F) which is consistent with paclitaxel.[25–27] Therefore, these results suggest the mechanism by which protuboxepin A induces tumor cell death is consistent with the hypothesis that protuboxepin A is a tubulin inhibitor.

2.2. Effects of protuboxepin A on tubulin networks

To further confirm our hypothesis that protuboxepin A is a tubulin inhibitor, we examined its effect on α-tubulin networks. Immunofluorescence showed that protuboxepin A, at a concentration of 80 or 160 μM, disrupted α-tubulin networks after 18 h without showing F-actin aggregation and disappearance (Figs. 2A and S4A). Protuboxepin A elicited a similar phenotype as paclitaxel, disrupting α-tubulin networks, increasing acetylated-tubulin signal, and inducing polyglutamylated-tubulin bleb formation; however, the induced distribution of γ-tubulin and nuclei were differed from paclitaxel as was the chromosome mislocalization in mitotic cells (Figs. 2B, S4B and S4C).[28–30] These results suggest that protuboxepin A disrupts α-tubulin networks resulting in round-up morphology and induction of subG$_1$ and G$_2$/M phase cells. From these observations we further hypothesized that protuboxepin A's disruption of α-tubulin networks leads to M phase arrest and chromosome misalignment.

2.3. Effects of protuboxepin A on cell cycle progression

We examined whether the protuboxepin A can induce M phase arrest and chromosome misalignment by treating Hep3B cells with 80 or 160 μM of protuboxepin A for 18 h. Then, we performed immunofluorescence to detect the phosphorylation of histone H3 at Ser10, an M phase marker.[31,32] Protuboxepin A increased the phosphorylation of histone H3 (Ser10) and induced chromosome misalignment in nuclei (Fig. 3A). Protuboxepin A increased the ratio of M phase cells from 6.24 ± 2.14% to 18.76 ± 2.87% and to 39.47 ± 6.55% at a concentration of 80 and 160 μM, respectively (Fig. 3B). Among mitotic Hep3B cells, protuboxepin A preferentially induced metaphase arrest in cells at a concentration of 160 μM (Fig. 3C). In contrast, paclitaxel mainly elicited prometaphase arrest in cells (Fig. 3C). Additionally, among metaphase cells, protuboxepin A treatment lead to a high percentage of cells with misaligned chromosomes (Fig. 3D). These results suggest that protuboxepin A-induced round-up morphology and increased subG$_1$ and M phase cells correlates with cell cycle metaphase arrest and chromosome misalignment in response to the disruption of tubulin function.

2.4. Protuboxepin A promotes tubulin polymerization and binds tubulin

Several tubulin inhibitors bind directly to tubulin and stabilize or inhibit tubulin polymerization.[33,34] Thus, we examined whether protuboxepin A interferes with tubulin polymerization in vitro. Protuboxepin A potentiated tubulin polymerization at a concentration of 80 and 160 μM (Fig. 4A). Moreover, protuboxepin A physically interacted with α,β-tubulin, and the affinity constants at several concentrations of protuboxepin A in the Octet system were computed by Global Fitting Analysis of a 1:1 binding interaction model (Fig. 4B).[35–37] The resulting kinetics constants are shown in Table 1. Protuboxepin A had the following dissociation equilibrium constant 7.13×10^{-5} M. These analyses demonstrate that protuboxepin A associates with α,β-tubulin, which may be necessary to induce metaphase arrest and chromosome misalignment through stabilized tubulin polymerization in Hep3B cells.

2.5. Microtubule dynamics effects of protuboxepin A

Next, we focused on the inhibition of microtubule dynamics by protuboxepin A. To investigated protuboxepin A's effects on microtubule dynamics, we used an EB1-EGFP expressing HeLa cells system.[38] EB1 (end binding 1) is a microtubule plus-end-tracking protein that localizes to microtubule plus ends where it modulates microtubule dynamics.[39,40] Fast turnover causes rapid loss of EB1-EGFP signals from non-polymerizing microtubule ends and rapid appearance of EB1-EGFP signals when microtubules start growing. We examined the effect of protuboxepin A on this system using image time-lapse analysis. After analyzing non-treatment mitotic cell, we added 80 or 160 μM protuboxepin A and incubated for 1 min. Then, we captured the effect of EB1-EGFP signals at 1 ms (milli second) intervals for 60 s in the same cell (Fig. S5A). EB1-EGFP signals were significantly and rapidly suppressed by protuboxepin A at a concentration of 160 and 80 μM in both polar opposites and cell equator (Figs. 5, S5B and Movies S1–6). In addition, protuboxepin A inhibited the growth of EB1-EGFP signals in interphase cells at 160 μM (Fig. S5C, D, Movies S7 and S8). These results demonstrate that protuboxepin A inhibits microtubule dynamics by preferentially microtubule-stabilizing in cells and specifically induces metaphase arrest and chromosome misalignment in tumor cells.

In conclusion, our study has revealed a new oxepin-containing diketopiperazine-type marine fungal metabolite, protuboxepin A that inhibits microtubule dynamics by tubulin stabilization. The resulting disruption of tubulin dynamics leads to metaphase arrest which in turn induces apoptosis. Prior to this report, no other oxepin-containing diketopiperazine compounds have been shown to stabilize or inhibit tubulin polymerization or induce of metaphase arrest.[41–44] Further chemical and biological analysis of protuboxepin A may lead to the development of a promising new microtubule inhibitor with a unique chemical structure compared that of therapeutics reagents currently under clinical trials.

3. Experiment methods

3.1. Materials

Protuboxepin A was isolated from a culture broth of the marine-derived fungus *Aspergillus* sp. SF-5044 previously described.[20]

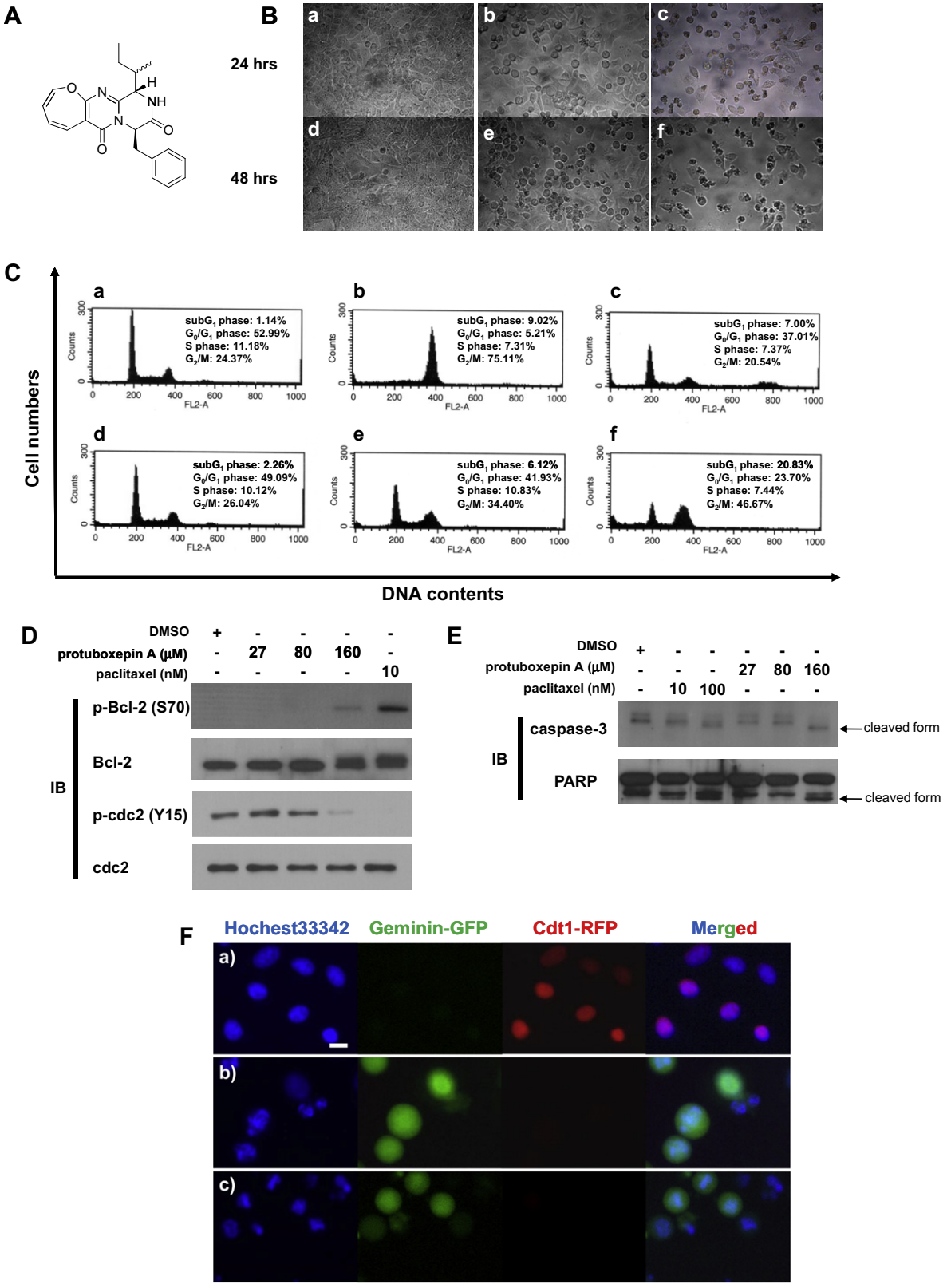

Figure 1. Activities of protuboxepin A in tumor cells. (A) The chemical structure of protuboxepin A. (B) Hep3B cells were treated for 24 or 48 h with 80 or 265 μM of protuboxepin A. Photographs of the sequential morphological change after treatment with (a, d): control, (b, e): 80 μM of protuboxepin A, (c, f): 265 μM of protuboxepin A. Observations were observed using a microscope at 200× power. (C) Effects of protuboxepin A on the distribution of DNA content in asynchronous Hep3B cells culture were analyzed by flow cytometry. Each panel showed (a): control for 24 h incubation, (b, c): Asynchronous Hep3B cells were treated with 0.5 μM of nocodazole (b) or cytochalasin D (c) for 24 h incubation. (d–f): Asynchronous Hep3B cells were treated with 27, 80, or 265 μM of protuboxepin A for 24 h, respectively. (D) Western blot showing the effect of protuboxepin A on the phosphorylation of Bcl-2 (Ser70) and cdc2 (Tyr15) in Hep3B cells following treatment of 27, 80, and 265 μM of protuboxepin A for 18 h. (E) Western blot showing the effect of protuboxepin A on the caspase-3 and PARP in Hep3B cells following treatment of protuboxepin A for 18 h. (F) Responses of HeLa cells by paclitaxel or protuboxepin A analyzed using the FUCCI (Fluorescent Ubiquitination-based Cell Cycle Indicator). Fluorescence observation of DNA (blue, Hochest33342), Geminin-GFP (green), and Cdt1-RFP (red) in HeLa cells treated for 18 h with (a): control, (b): 10 nM of paclitaxel, (c): 160 μM protuboxepin A in live cell image. Scale bar shows 20 μm.

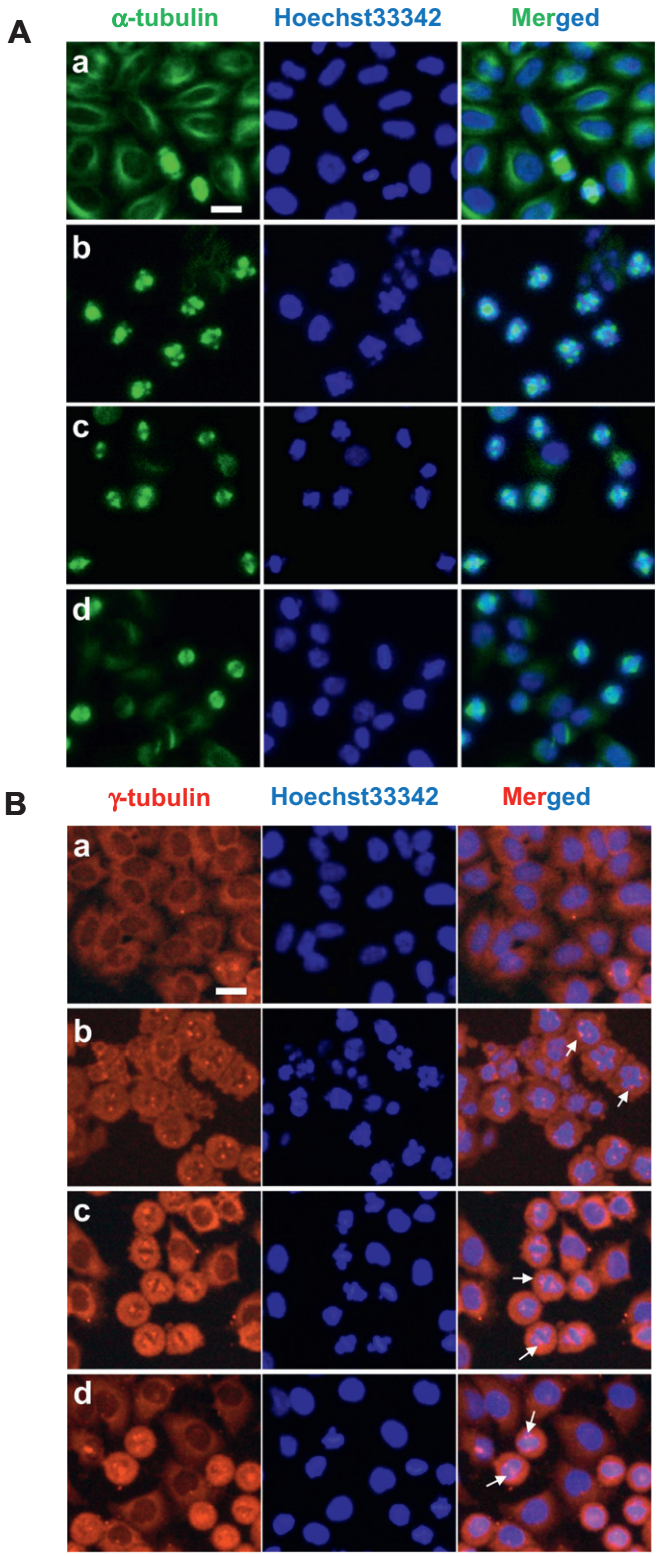

Figure 2. Profiles of tubulin and nucleus of Hep3B cells following the application of protuboxepin A. (A) Immunofluorescence staining of α-tubulin (green) and DNA (blue) treated for 18 h with (a): control, (b): 10 nM of paclitaxel, (c, d): 160 or 80 μM of protuboxepin A. (B) Immunofluorescence staining of γ-tubulin (red) and DNA (blue) treated for 18 h with (a): control, (b): 10 nM of paclitaxel, (c, d): 160 or 80 μM of protuboxepin A. White arrows indicate the localization of γ-tubulin in centrosomes. Scale bar shows 20 μm.

The tubulin stabilizing molecules paclitaxel and a tubulin destabilizing molecule nocodazole and vinblastine were purchased from Calbiochem (La Jolla, CA, USA). The actin polymerization inhibitor cytochalasin D was purchased from Sigma–Aldrich (St. Louis, MO, USA). Hoechst33342, Alexa Fluor® 488 conjugate anti-α-tubulin mouse monoclonal antibody and Alexa Fluor® 488 conjugate rabbit polyclonal IgG antibody were purchased from Invitrogen (Carlsbad, CA, USA). Cy3 conjugate anti-γ-tubulin rabbit polyclonal antibody, tubulin polygutamylated and acetylated (K40) mouse monoclonal antibodies were purchased from Abcam (Cambridge, MA, USA). Rabbit polyclonal antibodies against phospho-BCL-2 (S70), cdc2 (Y15), and Histone H3 (S10) were purchased from Cell Signaling Technology (Beverly, MA, USA), whereas the mouse monoclonal antibodies against BCL-2 and cdc2 were purchased from Santa Cruz Biotechnology (Santa Cruz, CA, USA) and Cell Signaling Technology, respectively. Rabbit polyclonal antibodies against caspase-3 and PARP were purchased from IMAGENEX (San Diego, CA, USA) and Santa Cruz Biotechnology, respectively. Blocking buffers and working concentrations of the above antibodies were prepared according to the manufacturers' instructions.

3.2. Cell morphology assay

Hep3B cells (human hepatocellular carcinoma cells) were grown in DMEM (Dulbecco's modified Eagle's medium) supplemented with 10% fetal bovine serum in the presence of 30 μg/mL penicillin and 42 μg/mL streptomycin under a humidified atmosphere of 5% CO_2 at 37 °C. Hep3B cells were seeded on microplate at a 3×10^4 cells/mL and cultured for 18 h. After treatment with compounds for 24 or 48 h, cell morphological changed were photographed with a Digital SLR camera D40 (Nikon Corporation, Tokyo, Japan). Observations were made using a microscope at 200× power.

3.3. Cell cycle analysis

Hep3B cells (2×10^4 cells/mL) were seeded on microplate and incubated overnight in the presence or absence of 500 nM of nocodazole or cytochalasin D and 27, 80 or 265 μM of protuboxepin A. After 24 h, cell cycle analyses were observed under BD FACSCalibur (Becton Dickinson, San Jose, CA) using CycleTESTTMPLUS reagents kit (Becton Dickinson).

3.4. Immunofluorescence staining

For immunofluorescence observation, Hep3B cells were seeded on microplate 3×10^4 cells/mL and cultured for 18 h. Then treated with 80 or 160 μM of protuboxepin A or 10 nM of paclitaxel for 18 h. Then the medium from the wells was excluded and the cells were fixed with 3.7% formaldehyde in PBS for 15 min then permeabilized for 5 min with 100% cold MeOH. The cells were washed with PBS-1% BSA [PBS containing 1% bovine serum albumin], and then blocked with 10% fetal bovine serum for 20 min. After being washed with PBS-0.1% BSA, the cells were treated with Alexa Fluor 488-conjugated α-tubulin antibody, Cy3 conjugated γ-tubulin antibody, or phospho-Histone H3 antibodies in PBS-0.1% BSA then placed in a humidified atmosphere of 5% CO_2 at 37 °C and incubated for 60 min. After being washed with PBS-0.1% BSA, the cells treated with phospho-Histone H3 antibody was incubated with Alexa Fluor 488-conjugated mouse or rabbit anti-IgG antibodies in PBS-0.1% BSA then placed in a room temperature and incubated for 60 min. After being washed with PBS-0.1% BSA, the cells were overlaid with Hoechst33342 for 5 min at room temperature and washed with PBS-0.1% BSA. The fluorescence was photographed with an invert microscopy ECLIPSE Ti-U (Nikon Corporation).

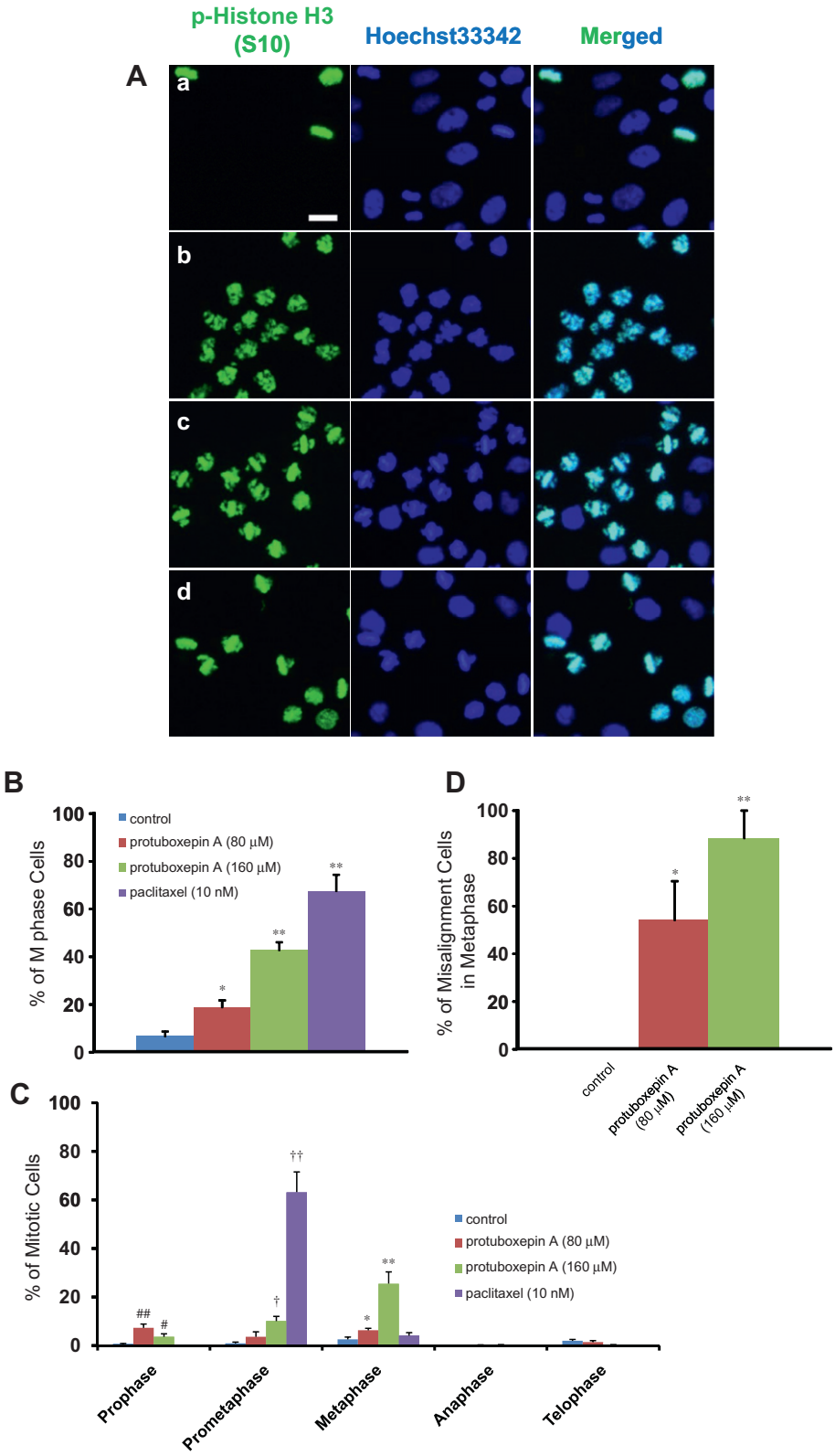

Figure 3. Protuboxepin A induced chromosome misalignment during metaphase. (A) Immunofluorescence staining of phospho-histone H3 (green) and DNA (blue) treated for 18 h with (a): control, (b): 10 nM of paclitaxel, (c, d): 160 or 80 μM of protuboxepin A. (B): M phase cells (phospho-histone H3 positive) were counted using an inverted microscopy. The statistical significance was determined using two groups two-tailed Student's *t*-test. *, P <0.0005; **, P <0.0001 were taken as the level of statistical significance. (C): Quantification of control, protuboxepin A or paclitaxel treatment during different mitotic stages. The statistical significance were determined using two groups two-tailed Welch's *t*-test on prophase and prometaphase. The statistical significance of metaphase was determined using two groups two-tailed Student's *t*-test. #, P <0.05; ##, P <0.005; †, P <0.01; ††, P <0.005; *, P <0.01; **, P <0.0001 were taken as the level of statistical significance. (D): Ratio of misalignment cells treated with protuboxepin A. The statistical significance was determined using two groups two-tailed Welch's *t*-test. * P <0.01; **, P <0.001were taken as the level of statistical significance. White bar shows 20 μm.

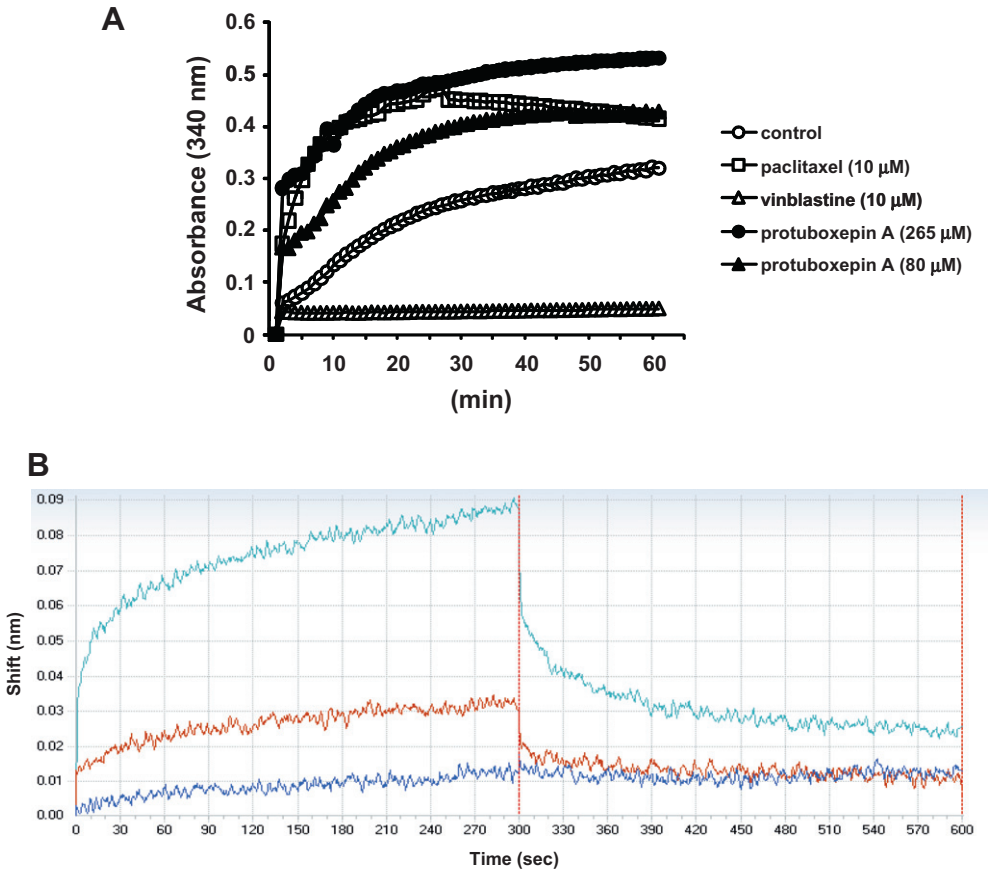

Figure 4. Analysis of protuboxepin A interaction with tubulin. The measurement of protuboxepin A effect on tubulin polymerization and binding affinity in vitro. (A) Effect of test compounds on the tubulin polymerization using 80 μM of protuboxepin A (closed triangles), 265 μM of protuboxepin A (closed circles), 10 μM of paclitaxel (open squares), 10 μM of vinblastine (open triangles), and 1% DMSO control (open circles) in a vitro assay. Absorbance at 340 nm was measured every 1 min for 60 min. (B) The binding interactions were measured using the ForteBio's Octet system for the interaction between protuboxepin A and biotin labeled tubulin (20 μg/mL) that was immobilized on a Super Streptavidin (SSA). The concentration of protuboxepin A varied from 2.65 (blue plot), 13.2 (red plot) and 26.5 μM (light blue plot).

Table 1
Direct binding kinetics for protuboxepin A binding tubulin on ForteBio's Octet System

Analyte	Ligand (tubulin)					
	K_{on} (1/Ms)	K_{on} Error	K_{off} (1/s)	K_{off} Error	K_A (1/M)	K_D (M)
Protuboxepin A	1.43×10^2	1.96×10	1.02×10^{-2}	2.43×10^{-4}	1.40×10^4	7.13×10^{-5}

The kinetic constants were calculated from the ForteBio's Octet System for the interaction between protuboxepin A and biotin-tubulin. K_{on}, association rate constant; K_{off}, dissociation rate constant; K_A, association equilibrium constant; K_D, dissociation equilibrium constant.

3.5. Western blotting

Hep3B cells (1×10^5 cells/mL) were seeded on 6-well plate and were untreated or exposed to various concentrations of protuboxepin A for 18 h. Ten nanomolar paclitaxel was used as a positive tubulin inhibitor control. Western blotting experiments were prepared as described previously.[45]

3.6. Observation of FUCCI (Fluorescent Ubiquitination-based Cell Cycle Indicator)

HeLa cells (5×10^4 cells/mL) were seeded on 12-well plate in DMEM (Dulbecco's modified Eagle's medium) supplemented with 10% fetal bovine serum in the presence of 30 μg/mL penicillin and 42 μg/mL streptomycin under a humidified atmosphere of 5% CO_2 at 37 °C and were exposed to 1×10^8 viral particles/mL of G_2/M reagent of geminin-GFP (Invitrogen) and G_1/S reagent of cdt1-RFP (Invitrogen) for 4 h at 27 °C. After being washed with PBS, the cells were treated with BacMan enhancer in 10% FBS-DMEM then placed in a humidified atmosphere of 5% CO_2 at 37 °C and incubated for 90 min. After incubation, the media was changed and exposed to 160 μM of protuboxepin A or 10 nM of paclitaxel in a humidified atmosphere of 5% CO_2 at 37 °C for 18 h. The fluorescence was photographed with an invert microscopy ECLIPSE Ti-U, respectively (Nikon Corporation).

3.7. In vitro tubulin polymerization assay

The tubulin polymerization assay kit was purchased from Cytoskeleton, Inc. (Denver, CO). Tubulin (>97% pure, Porcine) was mixed with general tubulin buffer (GTB; 80 mM PIPES pH 6.9, 2 mM $MgCl_2$, 0.5 mM EGTA, and 1 mM GTP) in a 96-well plate at 37 °C. Absorbance at 340 nm was measured every 1 min for 60 min by VERSAmax (Molecular Devices, Sunnyvale, CA).

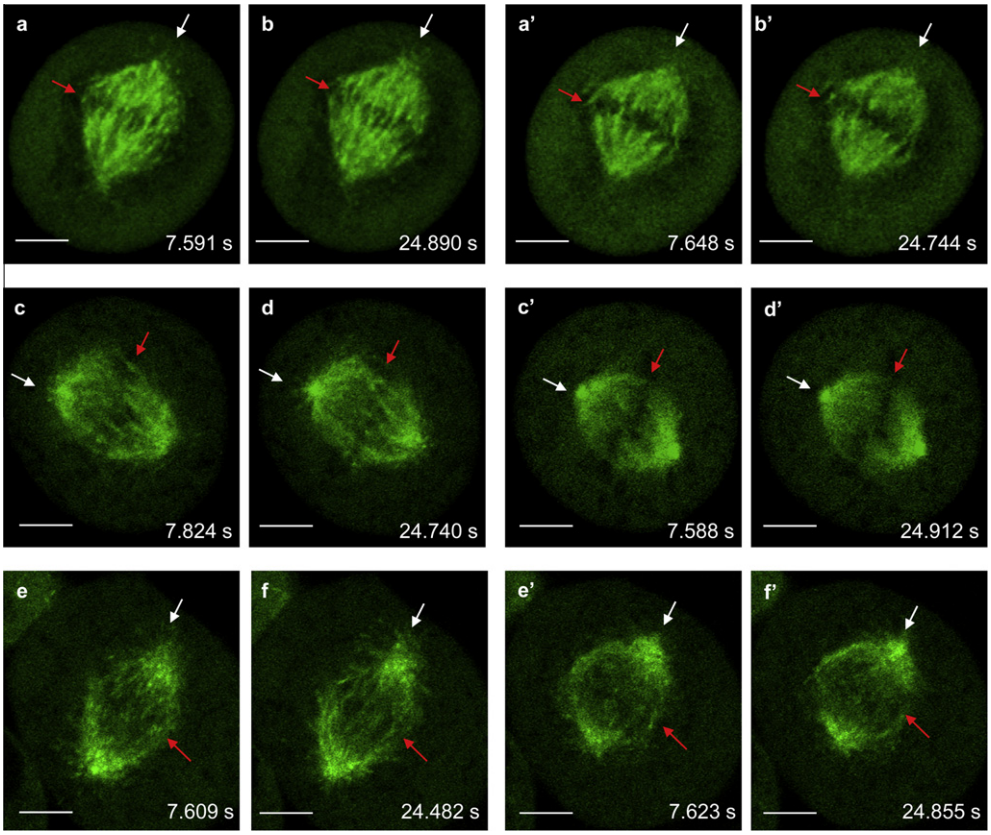

Figure 5. Protuboxepin A inhibition of microtubule dynamic as detected by growing microtubule plus ends. Analysis of the microtubule dynamics on mitotic cells. (a, b): Before treatment of 10 nM of paclitaxel, (a′, b′): After treatment of 10 nM of paclitaxel for 1 min, (c, d): Before treatment of 160 μM of protuboxepin A, (c′, d′): After treatment of 160 μM of protuboxepin A for 1 min, (e, f): Before treatment of 80 μM of protuboxepin A, (e′, f′): After treatment of 80 μM of protuboxepin A for 1 min. White and red arrows show the microtubule dynamics in bipolar and equator, respectively. Scale bars show 5 μm. See Movies S1–8.

3.8. Analyze of small molecule binding kinetics by octet system

The Octet RED (ForteBio, Inc., CA, USA) equipped with super streptavidin biosensor chips (ForteBio) was used for the analysis of small molecule protein interactions in fluidics free system. Super streptavidin biosensor chips were pre-wetted for 5 min in a modified GTB-buffer [80 mM PIPES pH 6.9, 2 mM $MgCl_2$, 0.5 mM EGTA, and 1 mM GTP]. 20 μg/mL of biotinylated-tubulin (>99% pure, Porcine brain, Cytoskeleton, Inc.) was immobilized on super streptavidin biosensor chips for 20 min at room temperature with 200 rpm rotated condition. After being washed with GTB-buffer (3 min at room temperature with 1000 rpm rotated condition), blocking was done using biocytin (ForteBio) (3 min at room temperature with 1000 rpm rotated condition) and equilibrating with GTB-buffer (3 min at room temperature with 1000 rpm rotated condition), then 2.65, 13.2 or 26.5 μM of protuboxepin A were loaded in sample well. Measurement of the association and the dissociation times were taken for 5 min at room temperature with 1000 rpm rotated condition. Analysis of the accurate and precise kinetic constants was performed by the Octet data analysis software version 6.3 (ForteBio).

3.9. Time-lapse analysis of the microtubule dynamic

EB1-EGFP was obtained from Addgene Inc. (Cambridge, MA, USA; Addgene plasmid 17234), and transferred (cloned into) into Lentiviral expressing vector. To generate Lentivirus, pHR-CMV VSV G, pHR-CMV 8.2 delta vpr and pHR′-CMV-SV40 puromycin based constructs described above. 293T cells were cotransfected with pHR-CMV VSV G, pHR-CMV 8.2 delta vpr and pHR′-CMV-SV40 puromycin based constructs described above. To select a lentivirus-integrated population, exponentially growing HeLa were infected with the viruses and treated with 2 μg/mL of puromycin for 2 days. EB1-EGFP signals were observed with a confocal laser scanning microscope LSM 710 (Carl Zeiss MicroImaging, Standort Göttingen-Vertrieb Deutschland, Germany) scanned image were analyzed by an ZEN2009 (Zeiss Efficient Navigation system) program. Optical images were captured at 1 ms (milli second) intervals after test compounds were added to 35 mm dishes and incubated for 1 min.

Acknowledgments

This research was supported by a grant from the Global R&D Center (GRDC) and World Class Institute (WCI) program through the National Research Foundation of Korea (NRF) funded from the Ministry of Education, Science and Technology of Korea, and a grant from KRIBB Research Initiative Program. We thank Professor Lynne Cassimeris for the gift of EB1-EGFP expression vector, Lehigh University. We are grateful to Dr. John Proctor (ForteBio, Inc.) for suggestions concerning the Octet system experiments. We thank Mr. Michael Molstad for proofreading the manuscript.

Supplementary data

Supplementary data associated with this article can be found, in the online version, at http://dx.doi.org/10.1016/j.bmc.2012.04.039.

References and notes

1. Jordan, M. A.; Wilson, L. *Nat. Rev. Cancer* **2004**, *4*, 253.
2. Jordan, A.; Hadfield, J. A.; Lawrence, N. J.; McGown, A. T. *Med. Res. Rev.* **1998**, *18*, 259.
3. Shah, M. A.; Schwartz, G. K. *Drug Resist. Updat.* **2000**, *3*, 335.
4. Rowinsky, E. K.; Tolcher, A. W. Antimicrotubule Agents. In *Cancer Principles and Practice*; Devita, V. T., Jr., Hellman, S., Rosenberg, S. A., Eds., 6th ed.; Lippincott Williams and Wilkins: Philadelphia, 2001; pp 431–452.
5. Rowinsky, E. K. *Annu. Rev. Med.* **1997**, *48*, 353.
6. Long, H. J. *Mayo Clin. Proc.* **1994**, *69*, 341.
7. Khan, N. U. *Nature* **1995**, *374*, 400.
8. Markman, M. *Oncologist* **2007**, *12*, 186.
9. Duflos, A.; Kruczynski, A.; Barret, J. *M. Curr. Med. Chem. Anticancer Agents* **2002**, *2*, 55.
10. Di Maio, M.; Krzakowski, M.; Fougeray, R.; Kowalski, D. M.; Gridelli, C. *Lung Cancer* **2012** Feb 21 [Epub ahead of print].
11. Usui, T.; Watanabe, H.; Nakayama, H.; Tada, Y.; Kanoh, N.; Kondoh, M.; Asao, T.; Takio, K.; Watanabe, H.; Nishikawa, K.; Kitahara, T.; Osada, H. *Chem. Biol.* **2004**, *11*, 799.
12. Bloom, K.; Joglekar, A. *Nature* **2010**, *463*, 446.
13. Peterson, J. R.; Mitchison, T. *J. Chem. Biol.* **2002**, *9*, 1275.
14. Crews, C. M.; Mohan, R. *Curr. Opin. Chem. Biol.* **2000**, *4*, 47.
15. Ledford, H. *Nature* **2010**, *468*, 608.
16. Kuznetsov, G.; Towle, M. J.; Cheng, H.; Kawamura, T.; TenDyke, K.; Liu, D.; Kishi, Y.; Yu, M. J.; Littlefield, B. A. *Cancer Res.* **2004**, *64*, 5760.
17. Yang, Y. R.; Kim, D. S.; Kishi, Y. *Org. Lett.* **2009**, *11*, 4516.
18. Kim, D. S.; Dong, C. G.; Kim, J. T.; Guo, H.; Huang, J.; Tiseni, P. S.; Kishi, Y. *J. Am. Chem. Soc.* **2009**, *131*, 15636.
19. Dong, C. G.; Henderson, J. A.; Kaburagi, Y.; Sasaki, T.; Kim, D. S.; Kim, J. T.; Urabe, D.; Guo, H.; Kishi, Y. *J. Am. Chem. Soc.* **2009**, *131*, 15642.
20. Lee, S. U.; Asami, Y.; Lee, D.; Jang, J. H.; Ahn, J. S.; Oh, H. *J. Nat. Prod.* **2011**, *74*, 1284.
21. Kawamura, K. I.; Grabowski, D.; Weizer, K.; Bukowski, R.; Ganapathi, R. *Br. J. Cancer* **1996**, *73*, 183.
22. Ling, Y. H.; Tornos, C.; Perez-Soler, R. *J. Biol. Chem.* **1998**, *273*, 18984.
23. Vantieghem, A.; Xu, Y.; Assefa, Z.; Piette, J.; Vandenheede, J. R.; Merlevede, W.; De Witte, P. A.; Agostinis, P. *J. Biol. Chem.* **2002**, *277*, 37718.
24. Huang, Y. T.; Huang, D. M.; Guh, J. H.; Chen, I. L.; Tzeng, C. C.; Teng, C. M. *J. Biol. Chem.* **2005**, *280*, 2771.
25. Sakaue-Sawano, A.; Kurokawa, H.; Morimura, T.; Hanyu, A.; Hama, H.; Osawa, H.; Kashiwagi, S.; Fukami, K.; Miyata, T.; Miyoshi, H.; Imamura, T.; Ogawa, M.; Masai, H.; Miyawaki, A. *Cell* **2008**, *132*, 487.
26. Sakaue-Sawano, A.; Ohtawa, K.; Hama, H.; Kawano, M.; Ogawa, M.; Miyawaki, A. *Chem. Biol.* **2008**, *15*, 1243.
27. Sakaue-Sawano, A.; Kobayashi, T.; Ohtawa, K.; Miyawaki, A. *BMC Cell Biol.* **2011**, *12*, 2.
28. Nováková, M.; Dráberová, E.; Schürmann, W.; Czihak, G.; Viklický, V.; Dr-aber, P. *Cell Motil. Cytoskeleton* **1996**, *33*, 38.
29. Uetake, Y.; Sluder, G. *Curr. Biol.* **2010**, *20*, 1666.
30. Cabral, F.; Wible, L.; Brenner, S.; Brinkley, B. R. *J. Cell Biol.* **1983**, *97*, 30.
31. Wei, Y.; Mizzen, C. A.; Cook, R. G.; Gorovsky, M.-A.; Allis, C. D. *Proc. Natl. Acad. Sci. U.S.A.* **1998**, *95*, 7480.
32. Wei, Y.; Yu, L.; Bowen, J.; Gorovsky, M. A.; Allis, C. D. *Cell* **1999**, *97*, 99.
33. Tahir, S. K.; Han, E. K.; Credo, B.; Jae, H. S.; Pietenpol, J. A.; Scatena, C. D.; Wu-Wong, J. R.; Frost, D.; Sham, H.; Rosenberg, S. H.; Ng, S. C. *Cancer Res.* **2001**, *61*, 5480.
34. Kondoh, M.; Usui, T.; Nishikiori, T.; Mayumi, T.; Osada, H. *Biochem. J.* **1999**, *340*, 411.
35. Abdiche, Y.; Malashock, D.; Pinkerton, A.; Pons, J. *Anal. Biochem.* **2008**, *377*, 209.
36. Papalia, G. A.; Leavitt, S.; Bynum, M. A.; Katsamba, P. S.; Wilton, R.; Qiu, H.; Steukers, M.; Wang, S.; Bindu, L.; Phogat, S.; Giannetti, A. M.; Ryan, T. E.; Pudlak, V. A.; Matusiewicz, K.; Michelson, K. M.; Nowakowski, A.; Pham-Baginski, A.; Brooks, J.; Tieman, B.-C.; Bruce, B. D.; Vaughn, M.; Baksh, M.; Cho, Y. H.; Wit, M. D.; Smets, A.; Vandersmissen, J.; Michiels, L.; Myszka, D.-G. *Anal. Biochem.* **2006**, *359*, 94–105.
37. Li, J.; Schantz, A.; Schwegler, M.; Shankar, G. *J. Pharm. Biomed. Anal.* **2011**, *54*, 286.
38. Matov, A.; Applegate, K.; Kumar, P.; Thoma, C.; Krek, W.; Danuser, G.; Wittmann, T. *Nat. Methods* **2010**, *7*, 761.
39. Goshima, G.; Nédélec, F.; Vale, R. D. *J. Cell Biol.* **2005**, *171*, 229.
40. Vitre, B.; Coquelle, F. M.; Heichette, C.; Garnier, C.; Chrétien, D.; Arnal, I. *Nat. Cell Biol.* **2008**, *10*, 415.
41. Cutler, H. G.; Springer, J. P.; Arrendale, R. F.; Arison, B. H.; Cole, P.-D.; Roberts, R. G. *Agri. Biol. Chem.* **1988**, *52*, 1725.
42. Belofsky, G. N.; Anguera, M.; Jensen, P. R.; Fenical, W.; Köck, M. *Chemistry* **2000**, *6*, 1355.
43. Sprogøe, K.; Manniche, S.; Larsen, T. O.; Christophersen, C. *Tetrahedron* **2005**, *61*, 8718.
44. Li, G. Y.; Yang, T.; Luo, Y. G.; Chen, X. Z.; Fang, D. M.; Zhang, G. L. *Org. Lett.* **2009**, *11*, 3714.
45. Asami, Y.; Kakeya, H.; Komi, Y.; Kojima, S.; Nishikawa, K.; Beebe, K.; Neckers, L.; Osada, H. *Cancer Sci.* **2008**, *99*, 1853.